Altered manganese homeostasis and manganese toxicity in Huntington's Disease striatal cell model are not due to defects in iron transport system.

By: B. Blairanne Williams, Gunnar F. Kwakye, Michal Wegrzynowicz, Daphne Li, Michael Aschner, Keith M. Erikson and Aaron B. Bowman

Williams, B.B., Kwakye, G.F., Wegrzynowicz, M., Li, D., Aschner, M., Erikson, K.M., Bowman, A.B. (2010) Altered manganese homeostasis and manganese toxicity in Huntington's Disease striatal cell model are not due to defects in iron transport system. *Toxicological Sciences* 117:169-179.

Abstract:

Expansion of a polyglutamine tract in Huntingtin (Htt) leads to the degeneration of medium spiny neurons in Huntington's disease (HD). Furthermore, the HTT gene has been functionally linked to iron (Fe) metabolism, and HD patients show alterations in brain and peripheral Fe homeostasis. Recently, we discovered that expression of mutant HTT is associated with impaired manganese (Mn) uptake following overexposure in a striatal neuronal cell line and mouse model of HD. Here we test the hypothesis that the transferrin receptor (TfR)–mediated Fe uptake pathway is responsible for the HD-associated defects in Mn uptake. Western blot analysis showed that TfR levels are reduced in the mutant STHdhQ111/Q111 striatal cell line, whereas levels of the Fe and Mn transporter, divalent metal transporter 1 (DMT1), are unchanged. To stress the Fe transport system, we exposed mutant and wild-type cells to elevated Fe(III), which revealed a subtle impairment in net Fe uptake only at the highest Fe exposures. In contrast, the HD mutant line exhibited substantial deficits in net Mn uptake, even under basal conditions. Finally, to functionally evaluate a role for Fe transporters in the Mn uptake deficit, we examined Mn toxicity in the presence of saturating Fe(III) levels. Although Fe(III) exposure decreased Mn neurotoxicity, it did so equally for wild-type and mutant cells. Therefore, although Fe transporters contribute to Mn uptake and toxicity in the striatal cell lines, functional alterations in this pathway are insufficient to explain the strong Mn resistance phenotype of this HD cell model.

Keywords: manganese | Huntington's disease | iron | neurotoxicity | transferrin receptors | nutrition | toxicology | medicine

Article:

Huntington's disease (HD) is an autosomal dominant neurodegenerative disorder predominantly afflicting the corpus striatum. Expansion of a glutamine encoding CAG triplet repeat in the

Huntingtin (HTT) gene causes HD (Walker, 2007). The medium spiny neurons of the corpus striatum are selectively lost during progression of HD. The pathophysiological basis of this selective pathology has not been fully elucidated. However, experimental evidence supports a number of underlying mechanisms including excitotoxicity and altered calcium signaling, mitochondrial dysfunction, oxidative stress, protein aggregation, loss of brain derived neurotrophic factor support, and others (Damiano et al., 2010; Graham et al., 2006, 2009; Heng et al., 2009; Roze et al., 2008; Strand et al., 2007; Zhang et al., 2008; Zuccato et al., 2001, 2005).

Metals have well-defined physiological functions within the brain, yet overexposures cause neurodegeneration and/or neuronal dysfunction (Bossy-Wetzel et al., 2004; Brown et al., 2005; Coppede et al., 2006). Additionally, many neurodegenerative disorders have been associated with altered metal homeostasis, emphasizing the importance of maintaining optimal metal levels for normal brain function. Finally, analysis of metal neurotoxicity has revealed similarities in the pathophysiological mechanisms of HD and other neurodegenerative disorders (Aschner et al., 2007; Fox et al., 2007; Molina-Holgado et al., 2007; Wright and Baccarelli, 2007). Both protein aggregation and oxidative stress, for example, have been implicated in the toxicity associated with HD and metal overexposure (Choi et al., 2007; Firdaus et al., 2006; Milatovic et al., 2009). Recognizing these similarities between HD and the toxicity of various metals, we performed a disease-toxicant interaction screen in a striatal neuronal cell line model of HD (Williams et al., 2010). This screen revealed a neuroprotective interaction between manganese (Mn) exposure and HD in which a striatal cell model expressing an expanded CAG repeat HTT allele showed decreased net Mn uptake following Mn exposure relative to wild-type cells. We also observed reduced net Mn uptake specifically into the striatum following systemic Mn exposure of a mouse model of HD (Williams et al., 2010). Importantly, the screen revealed that the phenotype is specific to Mn and does not occur with other metals known to induce protein aggregation or oxidative stress (e.g., Fe, Cu, and Zn). The mechanisms by which Mn exerts its cytotoxicity is likely similar in the presence of mutant HTT as exposure conditions yielding similar increases in cellular Mn burden in wild-type and mutant HTT cells exhibit similar cell death (Williams et al., 2010). With these data uncovering alterations in cellular Mn levels upon exposure, we focused on the pathways that contribute to cellular Mn transport.

Iron (Fe) and Mn transport and homeostasis are tightly linked. The major cellular Fe uptake pathway, the transferrin receptor (TfR)–mediated Fe uptake system, has been shown to mediate the uptake of Mn in the 3+ valence but has higher affinity for Fe(III) (Malecki et al., 1999). Not only can trivalent Mn be transported by the TfR but changes in Fe homeostasis can alter Mn homeostasis (Aschner and Gannon, 1994; Erikson et al., 2004; Fitsanakis et al., 2008; Garcia et al., 2006, 2007; Keefer et al., 1970). DMT1 (also known as NRAMP2), which transports Fe(II) and Mn(II), is regulated by cellular Fe status (Fleming et al., 1998; Gunshin et al., 2001; Lee et

al., 1998). Additionally, DMT1 plays a critical role in TfR-mediated Fe uptake, by mediating the release of Fe(II) from endocytic compartments (Fleming et al., 1998). Finally, the Fe exporter, ferroportin, has recently been shown to also contribute to Mn export (Yin et al., 2010). Evidence of coregulation in vivo and in vitro was reported in studies showing that both deficiency and repletion of either Fe or Mn is associated with changes in transport and homeostasis of the other metal (Erikson and Aschner, 2006; Erikson et al., 2002; Fitsanakis et al., 2008; Garcia et al., 2006, 2007; Zheng and Zhao, 2001).

A previous report utilizing a striatal neuronal cell line model of HD (STHdhQ111/Q111) found alterations in Fe signaling and increased expression of the TfR protein compared with a wild-type cells (STHdhQ7/Q7) (Trettel et al., 2000). Also, HD patients display elevated levels of Fe and copper (Cu) in the corpus striatum in both postmortem and functional magnetic resonance imaging studies (Bartzokis et al., 1999; Dexter et al., 1991; Fox et al., 2007). HTT, in partnership with two of its interacting protein, has also been shown to function in magnesium transport (Goytain et al., 2008). Expression of HTT is elevated in response to increasing Fe levels (Hilditch-Maguire et al., 2000). Additionally, in zebrafish, the embryonic lethality due to Htt inactivation has been attributed to a failure of appropriate utilization of Fe stores (Lumsden et al., 2007). Perhaps, most importantly, human mutations in a key Fe storage protein (L-ferritin) leads to neuroferritinopathy, a neurodegenerative condition with clinical similarities to HD (Curtis et al., 2001). Therefore, given our observations of decreased Mn uptake in both cellular and mouse models of HD and known functional links between Fe and Mn transport, we hypothesized that alterations in Fe homeostasis because of polyglutamine-expanded mutant HTT may underlie the decreased sensitivity to Mn toxicity and altered Mn transport. The objective of this study was to evaluate the contribution of alterations in Fe transport to the defect in Mn transport in the STHdhQ111/Q111 HD striatal cell model.

MATERIALS AND METHODS

Chemicals, reagents, and cell culture supplies.

Cell culture media and supplements were obtained from Mediatech (Manassas, VA) unless indicated. Cell lines were grown in Dulbecco's modified Eagle's medium with 10% fetal bovine serum (Atlanta Biologicals, Lawrenceville, GA, and Sigma, St Louis, MO), L-glutamine, 400 μg/ml G418, and Penicillin-Streptomycin. Mn(II) chloride was from Alfa Aesar (Ward Hill, MA). Fe(III) chloride was from Sigma. Buffers and solutions for assays: 3-(4,5-dimethylthiazol-2-yl)-2,5-diphenyltetrazolium bromide (MTT) salt (VWR, West Chester, PA), Sorenson's buffer (0.1M glycine, 0.1M NaCl2, pH 10.5), and DMSO (Sigma).

Cell culture and survival assays.

The clonal striatal cell lines—both mutant STHdhQ111/Q111 and wild-type STHdhQ7/Q7—were a generous gift from Marcy MacDonald, PhD (Massachusetts General Hospital, MA), and grown at 33°C (Trettel et al., 2000). Culture and assays were performed as previously described (Williams et al., 2010). In brief, STHdhQ111/Q111 and wild-type STHdhQ7/Q7 cells were plated at equal density the evening before treatment. Metals were added to the culture media the next morning, and the cells were exposed for 3 or 30 h. Cell viability was assessed in 24-well culture plates with the MTT assay according to established protocols (Ehrich and Sharova, 2000). Briefly, culture media was removed, and 500 µl of 0.5% MTT salt in minimal essential medium (MEM) (Invitrogen, Carlsbad, CA) containing FBS and Penicillin-Streptomycin was added to each well of the plate for 4 h. Next, the MEM was removed, and 200 µl of Sorenson's buffer diluted 1:8 in DMSO was added to the empty wells to dissolve the precipitate. The plates were returned to the incubator until all the MTT salt precipitate could no longer be visualized under a microscope. Samples were placed in a 96-well plate, and the absorbance was read at 570–590 nm. Cell survival data were normalized by genotype to the vehicle-only exposed control included in each independent sample set. The concentrations of Mn and Fe were based upon previously reported cell survival curves (Williams et al., 2010). In brief, we reported the maximal difference in survival and cellular response to Mn exposure between the two STHdh cell lines was at 40µM Mn (~50% difference in survival between wild-type and mutant cells). Furthermore, the 100µM Mn exposure was used because both cell lines exhibited clear Mn cytotoxicity at this concentration. It is also important to note that the amount of cell death in the mutant STHdh line exposed to 100µM Mn for ~30 h approximates the levels of cytotoxicity in the wild-type line at 40µM Mn. Additionally, under these exposure conditions, the amount of Mn accumulated within the cells is equal. Animals exposed to Mn can accumulate the metal in the stratum to levels as high as 70µM being reported (Aschner et al., 2005). The 600µM Fe(III) exposure was chosen because as the maximal exposure as it showed minimal cytotoxicity in both the wild-type and mutant STHdh cells.

Antibodies.

Primary antibodies used include: TfR (Invitrogen), DMT1 (+iron-responsive element (+IRE) and −IRE forms) (NRAMP24-S; ADI, San Antonio, TX), and actin (Developmental Studies Hybridoma Bank, Iowa City, IA). Appropriate peroxidase-conjugated secondary antibodies from Jackson Immunoresearch Laboratories (West Grove, PA) were used accordingly: IgG mouse, IgG rabbit, and IgM mouse.

Western blot.

Equal numbers of wild-type and mutant STHdh cells were plated onto 10-cm2 plates, treated with Mn(II) chloride for 3 or 30 h, and harvested by trypsinization. The cell pellets were lysed in RIPA buffer (50mM Tris, 150mM NaCl2, 0.1% SDS, 1.0% Nonidet 40, 12mM deoxycholic acid, 1× protease inhibitor cocktail [Sigma], and 1× phosphatase inhibitor cocktails I and II [Sigma]) and loaded by equal cell number or equal protein for SDS-PAGE. Western blots were visualized with Thermo Scientific Pierce Supersignal West Dura Extended Duration Chemiluminescent Substrate (Waltham, MA) on an Ultralum Omega 12iC (Claremont, CA). Measurements of integrated density of protein bands were performed using ImageJ (NIH), with background correction calculated using a signal ratio error model, as described (Kreutz et al., 2007). Calculations of relative signal were normalized to untreated wild-type or mutant sample for each set, as indicated.

Graphite furnace atomic absorption spectroscopy.

Total Fe and Mn concentrations were measured with graphite furnace atomic absorption spectroscopy (GFAAS) (Varian Inc., AA240, Palo Alto, CA). STHdh cells grown in 10-cm2 plate were cultured and treated as described above for cell viability assays, harvested by trypsinization, total cell number was then counted by hemacytometer, the cell pellet was washed multiple times in PBS, and finally flash-frozen until analysis. To increase sensitivity for determination of basal Mn levels, cells from two 10-cm2 plates were combined before GFAAS analysis. For analysis, cell pellets were thawed and digested in 200-µl ultrapure nitric acid for 24 h in a sandbath (60°C). Mn and Fe contents were determined by the following protocol: A 20-µl aliquot of the digested sample was brought to 1 ml total volume with 2% nitric acid for analysis. Bovine liver (NBS Standard Reference Material, USDC, Washington, DC) (10 µg Mn/g; 184 µg Fe/g) was digested in ultrapure nitric acid and used as an internal standard for analysis (final concentration 5 µg Mn/l; 92 µg Fe/l) as published previously (Anderson et al., 2009). Because of the small size of the cell pellets and genotype-specific differences in protein content, cellular Mn and Fe levels were calculated by normalizing to cell number for each sample (i.e., fmol metal/100 cells). To enable comparisons with other published values, we also report estimated metal content values for some of our measures expressed in calculated units of nmol Mn per mg protein. These values were calculated post hoc by measuring total cellular protein levels in wild-type (0.207 mg protein/1 × 106 cells) and mutant cell lines (0.162 mg protein/1 × 106 cells) using the Bio-Rad DC protein assay (Bio-Rad, Hercules, CA) and hemacytometer counts. The change in net metal uptake above basal levels was calculated by subtracting the mean total cellular metal content (fmol metal/100 cells) under basal cell culture conditions by the mean total cellular metal content (fmol metal/100 cells) following a 30-h exposure.

Statistical analysis.

Univariate and repeated-measures ANOVA tests were performed using SPSS 18 software (IBM, Inc., Chicago, IL). Post hoc analysis and pairwise comparisons were done using Microsoft Excel (Microsoft, Redmond, WA) by Student's t-tests (two tailed) or testing for nonoverlap of the 95% confidence interval for normalized ratios; error bars are expressed as SEM. SDs for the change in net metal uptake above basal levels were calculated by appropriate propagation of uncertainty calculations for subtraction of sample means, with significant differences between wild-type and mutant cells evaluated by nonoverlap of the 95% confidence interval.

RESULTS

Decreased Levels of TfR and Mn Responsiveness in Mutant STHdh Cells

To begin our investigation, we examined the levels of TfR between wild-type and mutant STHdh cell lines exposed for 3 h to varying concentrations on Mn. We used samples previously examined for AKT activation (Williams et al., 2010), which showed a selective deficit in Mn-dependent activation in the mutant STHdhQ111/Q111 versus wild-type STHdhQ7/Q7 cells. Western blot analysis of these samples revealed a modest ∼20% decrease in TfR levels in mutant STHdhQ111/Q111 cells irrespective of exposure (Fig. 1). ANOVA found a significant effect of genotype ($p = 0.001$) but no effect of treatment nor a genotype-by-treatment interaction. The levels of TfR and other essential components of the Fe signaling pathway are altered in response to Mn intoxication (Kwik-Uribe and Smith, 2006; Kwik-Uribe et al., 2003; Li et al., 2005; Lu et al., 2005; Wang et al., 2008) as well as by mutant alleles of HTT (Hilditch-Maguire et al., 2000; Simmons et al., 2007; Trettel et al., 2000). To test the hypothesis that a 3-h Mn exposure is insufficient to observe an alteration in total TfR levels, we examined a 30-h exposure of cells to 40μM Mn(II) chloride and measured protein levels. This exposure was selected based on our previous work demonstrating a substantial difference in Mn toxicity and Mn uptake between wild-type and mutant cells at this duration and concentration, yet low enough toxicity in the mutant as to enable sufficient survival for quantification of protein levels (Williams et al., 2010). Western blot analysis confirmed decreased TfR levels in the mutant line and revealed an increase in total TfR levels in Mn-exposed cells (Fig. 2). ANOVA found a significant effect of genotype ($p < 0.001$) as well as Mn treatment ($p = 0.003$) on TfR levels, with a trend for a genotype-by-treatment interaction ($p = 0.18$). Post hoc pairwise comparisons demonstrated a significant decrease in TfR levels between wild-type and mutant cells under both basal and Mn exposure conditions ($p < 0.05$). In addition, with the 30-h exposure to 40μM Mn, we observed an increase in cellular levels of TfR in the wild-type cell line ($p < 0.05$). However, the change was not significant in the mutant STHdhQ111/Q111 cell line after exposure to Mn, consistent with a decreased responsiveness of the mutant STHdhQ111/Q111 cell line to Mn exposure.

Figures 1 & 2 are omitted from this formatted document.

DMT1 Levels Are Unchanged in HD Mutant Cell Line

Bioavailability of endocytosed transferrin-bound Fe is mediated in part by the proton-coupled metal transporter, divalent metal transporter 1 (DMT1). To determine if changes in TfR levels correspond to alterations in cellular DMT1 levels, we used Western blot analyses to measure total protein levels in vehicle and 30-h 40μM Mn-exposed cells (Fig. 3). ANOVA found no significant difference in DMT1 levels as a measure of genotype, Mn exposure, or two-way interaction for treatment × genotype. There was a slight trend ($p = 0.098$) toward increased DMT1 levels in mutant cells overall—but this was not statistically significant.

Figure 3 is omitted from this formatted document.

Net Fe Accumulation after Fe Exposure Is Moderately Reduced in HD Mutant Cells

Our previously published data examining total Fe accumulation following Mn exposure showed a statistical trend ($p = 0.118$) for a two-way interaction between Mn exposure and genotype (Williams et al., 2010), in which an increase in Fe levels with Mn exposure was seen only in wild-type cells. Given the reduced expression of TfR in the mutant striatal cells (Fig. 1), we tested the hypothesis that mutant STHdhQ111/Q111 cells would show reduced Fe accumulation following Fe exposure versus wild-type cells. We compared total cellular Fe levels measured by GFAAS between wild-type and mutant cells under either basal conditions or exposure to 100 or 600μM Fe(III) chloride for 30 h (Fig. 4A). Fe levels were chosen to enable a comparable concentration with our 100μM Mn exposures and a high concentration (600μM Fe(III)) to stress the Fe pathway maximally. Mutant STHdhQ111/Q111 cells showed a slight decrease (~30%) in Fe accumulation versus wild-type cells under 100μM Fe exposures, but this difference was not significant ($p = 0.151$). However at 600μM Fe exposure, a significant difference ($p = 0.038$) was seen in which mutant STHdhQ111/Q111 cells accumulated approximately 40% less Fe than wild-type cells (Fig. 4A; 600μM).

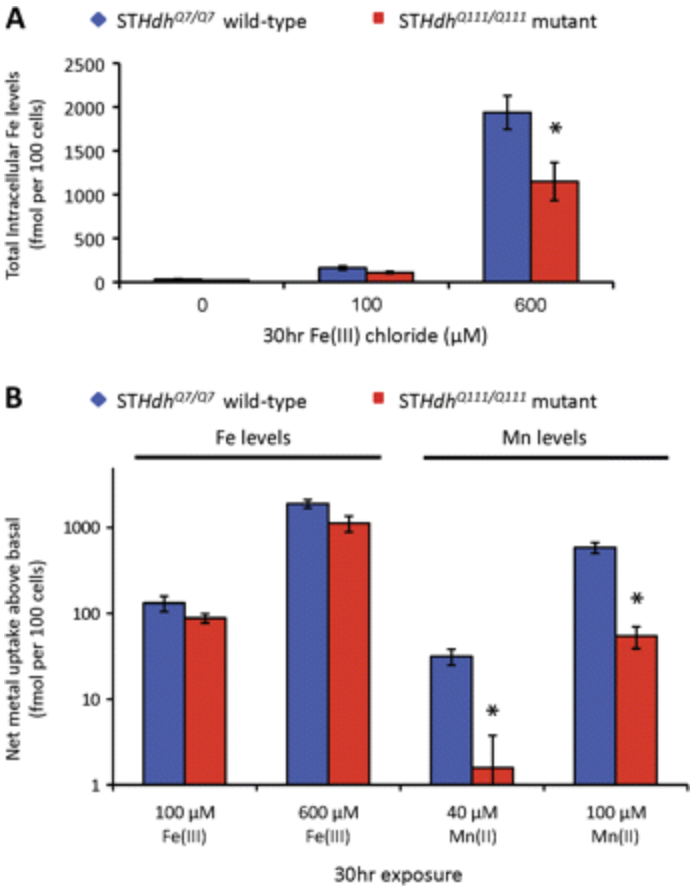

FIG. 4.

Net Fe uptake is reduced in the HD striatal cells. (A) Measurement of total intracellular Fe levels in ST*Hdh*$^{Q7/Q7}$ or ST*Hdh*$^{Q111/Q111}$striatal cell lines (as indicated) after application of the indicated concentrations of Fe(II) chloride for 30 h (n = 3 to 5). Mean values (±SEM) are plotted on a linear scale. (*B*) Comparisons of net Fe uptake versus net Mn uptake above basal levels (vehicle control) in ST*Hdh*$^{Q7/Q7}$ (blue) versus ST*Hdh*$^{Q111/Q111}$ (red) cells following a 30-h exposure to these metals. Calculations are derived from Fe data in (Fig. 4A) and previously published Mn data (Williams *et al.*, 2010). Data expressed as the absolute difference (±SEM) between metal-exposed and vehicle-exposed cells (n = 3–5), plotted on $\log_{10}$ scale. "*" Indicates a significant difference in net metal uptake ($p < 0.05$, using 95% confidence intervals) between wild-type and mutant cells.

Magnitude of Mn Uptake Deficit in HD Mutant Cells Greatly Exceeds Fe Uptake Deficit

To explore the magnitude of the differences between net Mn versus net Fe accumulation in the HD cell model, we compared the degree of accumulation for each metal above basal levels

between wild-type and mutant cells after exposure to low and high levels of the metal (Fig. 4B). Basal cellular Fe levels are approximately 10-fold higher than basal cellular Mn levels in wild-type cells (Fig. 5). To adjust for this difference, we examined the differences in fold-change of cellular metal content between Fe and Mn following exposure (i.e., the ratio of Fe levels following Fe exposure over basal Fe levels versus the ratio of Mn levels following Mn exposure over basal Mn levels). We found that the proportional rise in metal content in wild-type cells is similar between 100μM Fe (5.6-fold ± 2.3 SEM) and 40μM Mn (5.8-fold ± 1.2 SEM) exposures. Likewise the proportional rise was similar between 600μM Fe (68-fold ± 25 SEM) and 100μM Mn (90-fold ± 17 SEM) exposures. Considering this in another way, we examined the absolute rise in metal above basal cellular levels (i.e., the difference between metal levels postexposure and basal levels). We found that the absolute increase in cellular Fe levels for 100μM Fe exposure (+132 fmol Fe per 100 cells) was between the range of absolute net Mn uptake for the 40μM Mn exposure (+32 fmol Mn per 100 cells) and the 100μM Mn exposure (+587 fmol Mn per 100 cells) in wild-type cells (Fig. 4B). Thus, the Fe and Mn exposures examined led to comparable changes in cellular metal levels in wild-type cells.

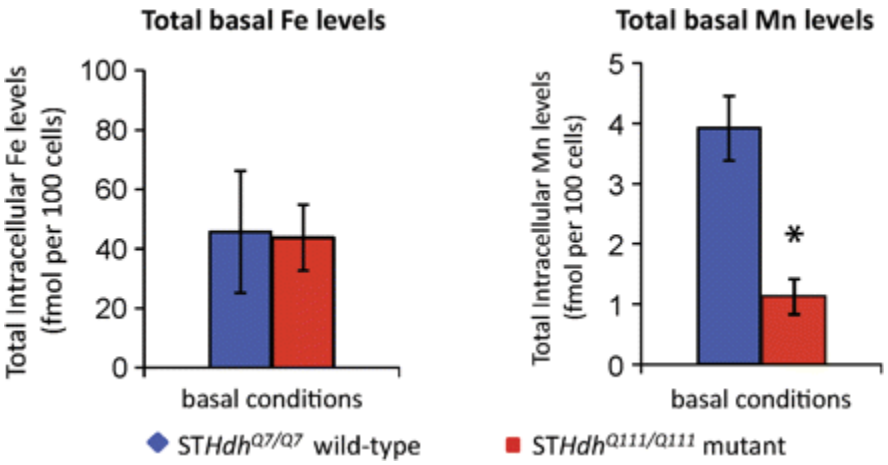

FIG. 5.

Basal Mn deficiency in HD striatal cells. Measurement of total intracellular Fe and Mn by GFAAS of cells collected from two 10-cm^{2}plates per sample of ST*Hdh*$^{Q7/Q7}$ or ST*Hdh*$^{Q111/Q111}$ cells (as indicated). Cells grown under standard culture conditions without supplemented Mn(II) or Fe(III). The mean total metal levels (±SEM) are plotted as indicated. "*" Indicates a significant difference in measured metal levels ($p < 0.05$, *t*-test) between wild-type and mutant cells.

Given comparable metal transport activity between these Fe and Mn exposures, we compared net metal uptake between wild-type and mutant HD cells. We found a subtle decrease (<40%), which did not reach statistical significance, in net Fe uptake in mutant HD cells relative to wild type for both Fe exposures (Fig. 4B). In contrast, we found a substantial and significant decrease

(>90%) in net Mn uptake in mutant HD cells relative to wild type for both the 40 and 100μM Mn exposures (Fig. 4B).

Mutant HD Striatal Cells Exhibit a Basal Mn Deficiency

The analysis described above revealed that differences in TfR levels and Fe accumulation upon exposure do not correspond with a significant decrease in total cellular Fe content under basal culture conditions (Fig. 4A). Given the striking deficit in net Mn uptake, we sought to better evaluate the basal levels of Mn in the mutant ST*Hdh*$^{Q111/Q111}$ cells because extracted Mn levels were near the detection limit of the GFAAS in our previously published study (Williams *et al.*, 2010). To increase the accuracy in measurement of basal Mn levels, we pooled plates of wild-type or mutant cells grown under basal culture conditions before GFAAS analysis. GFAAS measurements of total Fe and Mn levels confirmed no difference in basal Fe levels but revealed a substantial (~4-fold) and significant ($p = 0.004$) deficiency in basal Mn levels in the mutant ST*Hdh*$^{Q111/Q111}$ cells (Fig. 5). Basal Mn levels in the wild-type cells were 3.92 fmol per 100 cells (~0.189 nmol Mn per mg protein), whereas in the mutant cells basal levels were lower at 1.12 fmol per 100 cells (~0.069 nmol Mn per mg protein).

Saturating Levels of Fe Block Mn Toxicity Independent of HD Genotype

To address more directly the role of Fe transport and its potential contribution to the *HTT*-Mn gene-environment interaction, we examined the toxicity of Mn in the presence of saturating levels of Fe(III), 600μM (Fig. 6). At 600μM Fe(III), cell survival was significantly decreased in a dose-dependent manner as determined from previously published data (Williams *et al.*, 2010). We reasoned that at high levels of Fe(III), the TfR pathway would be saturated, thereby limiting the transport of other metals through this pathway. Thus, we expected that high levels of Fe(III) would decrease the toxicity of Mn(II) taken up by this Fe-saturable transport system but would have minimal influence on Mn toxicity driven by uptake systems that are independent of Fe. Furthermore, if changes in the activity of Fe transport pathways substantially contributed to the changes in net Mn uptake in the HD cell model, then we would expect saturating levels of Fe(III) to suppress the *HTT*-Mn gene-environment interaction. We report that saturating amounts of Fe(III) diminish Mn toxicity in both cell lines (Fig. 6A). A three-factor repeated-measures ANOVA (Fig. 6B) found a significant effect of genotype ($p = 0.035$), Mn exposure ($p < 0.001$), and a two-way interaction between genotype and Mn exposure ($p = 0.017$), recapitulating the gene-environment interaction we have previously reported (Williams *et al.*, 2010). The ANOVA revealed no significant effect of Fe exposure nor a significant two-way interaction for Fe exposure and genotype, indicating no differential sensitivity to Fe toxicity between the two cell lines, also as previously reported (Williams *et al.*, 2010). However, a significant two-way interaction between Fe-exposure and Mn-exposure was observed ($p = 0.004$), demonstrating that Fe exposure reduces Mn toxicity. Importantly, the ANOVA also found no significant three-way interaction of genotype by Mn exposure by Fe exposure (Fig. 6B). This indicates that although Fe reduced Mn toxicity, it did so equally for wild-type and mutant cells. Controlling for Fe

toxicity, the difference in percent cell survival between wild-type and mutant cells following a 30-h 100μM Mn(II) exposure was similar and independent of coexposure to 600μM Fe(III) (Fig. 6C).

Figure 6 has been omitted from this formatted document.

DISCUSSION

We tested the hypothesis that alterations in Fe transport contribute to a defect in Mn transport that confers resistance to Mn toxicity in a striatal cell line model of HD (Trettel *et al.*, 2000; Williams *et al.*, 2010). Our data demonstrate alterations in the TfR-mediated Fe transport pathway and differences in cellular Fe uptake with overexposure in mutant ST*Hdh*$^{Q111/Q111}$ cells compared with wild type (Figs. 1, 2, and 4A). However, this deficit in Fe uptake does not translate into a significant difference in net Fe uptake above basal levels between wild-type and mutant cells exposed to high levels of Fe (Fig. 4B). Thus, it is likely that compensatory changes are occurring to maintain Fe homeostasis. In contrast, the rise in net Mn levels above basal levels in mutant ST*Hdh*$^{Q111/Q111}$ cells treated with Mn is substantially less than what occurs in wild-type cells. Furthermore, we find that saturating Fe(III) levels partially suppress Mn(II) toxicity, consistent with a contribution of cellular Fe transport systems in regulating Mn trafficking (Fig. 6).

Despite a role for Fe-transport systems in Mn uptake, we found that both mutant and wild-type cells are equally protected from Mn toxicity by high levels of Fe. The toxicity of Fe(III), Cu(II), Pb(II), Co(II), Zn(II), and Ni(II) were previously reported to be similar between wild-type and mutant cells (Williams *et al.*, 2010). Also mutant ST*Hdh*$^{Q111/Q111}$ cells are more sensitive to Cd(II) (Williams *et al.*, 2010). Each of these metals are substrates for DMT1, some with higher affinities than Mn(II) (Gunshin *et al.*, 1997). Thus, coupled with evidence reported here that total DMT1 levels are unchanged (Fig. 3), it is unlikely that DMT1 is responsible for the difference in Mn transport in the HD models. In addition to DMT1, the ZIP8 family of transporters, metal/bicarbonate ion symporters, have been shown to transport Fe and Mn (Girijashanker *et al.*, 2008; He *et al.*, 2006;Liuzzi *et al.*, 2006). But, again as Zn and Cd are also transported by this family of transporters, the ZIP8 family is unlikely to contribute to the Mn accumulation defect in our HD model. Altogether, these analyses strongly argue that defects in known Fe transport pathways are not sufficient to explain the HD-Mn disease-toxicant interaction.

Alterations in Fe transport and Fe homeostasis have previously been reported in HD experimental models and patients (Bartzokis *et al.*, 1999;Dexter *et al.*, 1991; Fox *et al.*, 2007; Trettel *et al.*, 2000). We find that total TfR levels are decreased in the mutant ST*Hdh*$^{Q111/Q111}$ cells compared with wild-type ST*Hdh*$^{Q7/Q7}$ cells (Figs. 1 and 2). Previous studies with early passage lines by Marcy MacDonald and colleagues reported increased TfR levels and increased transferrin uptake activity (Trettel *et al.*, 2000). In contrast, the cells utilized in this study are of a later passage, and based on data here, the mutant cells seem to have reduced TfR

levels, yet normal cellular Fe uptake relative to the wild-type cells. Indeed, despite reduced levels of TfR protein in the mutant cells, total Fe levels under basal culture conditions between wild-type and mutant cells are not significantly different (Figs. 4 and 5). Furthermore, time in culture (perhaps related to cell density) also appears to influence TfR levels—compare difference in TfR levels in the 3-h exposure condition (Fig. 1) with the 30-h exposure condition (Fig. 2). Thus, it is likely that the decreased TfR levels in the mutant cells is a reflection of regulatory actions by the cells to maintain cellular Fe homeostasis.

We observe a significant increase in total TfR levels with the 30-h 40μM Mn exposure in wild-type cells, but not mutant cells. Furthermore, this increase does not occur as early as 3 h after exposure, even at very high levels of Mn. Increased TfR levels following Mn exposure has been reported in both animal and cellular models (Garcia *et al.*, 2006; Li *et al.*, 2005; Zheng *et al.*, 1999). The failure to significantly elevate TfR levels in the mutant cells (Fig. 2) was concurrent with decreased Mn uptake (Fig. 4B). Thus, the regulatory mechanisms that link Mn exposure to elevated TfR levels are likely dependent on intracellular rather than extracellular Mn.

We find that the ST*Hdh* striatal cell model of HD exhibits a substantial deficiency in total cellular Mn content under basal culture conditions (Fig. 5). This raises the possibility that the disease-causing allele of *HTT* may lead to a defect in neuronal Mn homeostasis. Thus, in addition to the reported alterations in Fe and Cu levels in HD (Bartzokis *et al.*, 1999;Dexter *et al.*, 1991), our observations suggest that Mn changes may also occur. Only one study that we are aware of has examined Mn levels in HD patient brains, reporting no significant alterations in brain Mn levels; however, this study examined only four HD striatal samples and therefore was statistically underpowered to detect small changes (Dexter *et al.*, 1991). Our earlier study reported decreased Mn uptake after subcutaneous Mn exposure in the presymptomatic YAC128Q mouse model of HD, specifically in the striatum (Williams *et al.*, 2010). However, we did not detect a deficiency in basal Mn levels. Future studies should evaluate whether examining specific cell types (e.g., neurons versus glia) or disease progression (e.g., older animals) may reveal a change in basal Mn levels.

There are few reports on the phenotypes because of Mn deficiency in adult animals, but Mn is required for the proper function of many enzymes key to brain function (e.g., glutamine synthetase [GS], pyruvate carboxylase, superoxide dismutase 2 [SOD2], arginase, and serine/threonine protein phosphatase) (Applebury *et al.*, 1970; Eid *et al.*, 2008; Ensunsa *et al.*, 2004; Greger, 1999; Tholey *et al.*, 1988a, 1988b;Wedler *et al.*, 1994). Several of these Mn-dependent enzymes have direct links to HD. For example, the activity of GS, which metabolizes glutamate, an excitatory neurotransmitter, to glutamine, is decreased in the corpus striatum of HD patients (Butterworth, 1986; Carter, 1981). However, other glial-specific activities are elevated, suggesting that GS activity is not lost because of general glial cell loss (Butterworth, 1986). Importantly, expression of mutant *htt* in astrocytes and reductions in GS activity are both associated with increased excitotoxicity (Fernandes *et al.*, 2007; Shin*et al.*, 2005; Zeron *et al.*, 2001). Additionally, deficiencies in SOD2 have been shown to increase sensitivity to 3-

nitropropionic acid (3-NPA), a toxicant that has been used to model HD (Andreassen *et al.*, 2001; Beal *et al.*, 1993). Of note, the mutant ST*Hdh*$^{Q111/Q111}$ cells are hypersensitive to 3-NPA (Trettel *et al.*, 2000; Williams *et al.*, 2010). Finally, the Mn-dependent enzyme arginase regulates the final step of the urea cycle in liver; both HD patients and mouse models have deficiencies in the urea cycle (Chiang *et al.*, 2007; Stoy *et al.*, 2005). Thus, alteration in Mn homeostasis has the potential to influence a variety of enzymes whose activities have clear pathophysiological links to HD.

In summary, expression of mutant *HTT* was found to alter Mn homeostasis in a mouse striatal cell model of HD. Saturating Fe exposure reduced Mn toxicity, indicating a clear link between Fe transport pathways and regulation of cellular Mn levels. However, altered Mn homeostasis was not explained by confirmed HD-associated defects in Fe transport pathways because Fe protected against Mn cytotoxicity equally in wild-type and mutant cells. Therefore, some other Mn uptake, storage, or efflux mechanisms must be altered in this HD model and account for the substantial deficit in net Mn uptake. Future studies will be needed to examine the cellular basis for the Mn transport defect and the potential role of HTT (direct or indirect) in regulating cellular Mn levels. Given the decreased striatal Mn uptake following Mn exposure in the YAC128Q HD mouse model we have previously reported (Williams *et al.*, 2010), future studies will also need to examine the role of these Mn transport pathways*in vivo*. Interestingly, there is a precedent of pathophysiological interactions between metals such as Mn and proteins associated with neurodegenerative diseases (Choi *et al.*, 2006, 2007, 2010; Gitler *et al.*, 2009). Thus, changes in Mn homeostasis because of the disease-causing allele of *HTT* may potentially contribute to the selective degeneration of medium spiny neurons in the corpus striatum that occurs in HD.

FUNDING

National Institutes of Health (RO1 ES10563 to M.A., R15 NS061309-01 to K.M.E, and RO1 ES016931 to A.B.B.).

Acknowledgments

We would like to thank Marcy MacDonald, PhD (Massachusetts General Hospital), for generous gifts of the ST*Hdh* cell lines. We also thank Roger Colbran, PhD, and Doug Mortlock, PhD (Vanderbilt University), for insightful discussions.

References

Anderson J, Fordahl S, Cooney P, Weaver T, Colyer C, Erikson K. Extracellular norepinephrine, norepinephrine receptor and transporter protein and mRNA levels are differentially altered in the developing rat brain due to dietary iron deficiency and manganese exposure. Brain Res. 2009;1281:1-14.

Andreassen O, Ferrante R, Dedeoglu A, Albers D, Klivenyi P, Carlson E, Epstein C, Beal M. Mice with a partial deficiency of manganese superoxide dismutase show increased vulnerability to the mitochondrial toxins malonate, 3-nitropropionic acid, and MPTP. Exp. Neurol. 2001;167:189-195.

Applebury M, Johnson B, Coleman J. Phosphate binding to alkaline phosphatase. Metal ion dependence. J. Biol. Chem. 1970;245:4968-4976.

Aschner M, Erikson K, Dorman D. Manganese dosimetry: species differences and implications for neurotoxicity. Crit. Rev. Toxicol. 2005;35:1-32.

Aschner M, Gannon M. Manganese (Mn) transport across the rat blood-brain barrier: saturable and transferrin-dependent transport mechanisms. Brain Res. Bull. 1994;33:345-349.

Aschner M, Guilarte T, Schneider J, Zheng W. Manganese: recent advances in understanding its transport and neurotoxicity. Toxicol. Appl. Pharmacol. 2007;221:131-147.

Bartzokis G, Cummings J, Perlman S, Hance D, Mintz J. Increased basal ganglia iron levels in Huntington disease. Arch. Neurol. 1999;56:569-574.

Beal M, Brouillet E, Jenkins B, Ferrante R, Kowall N, Miller J, Storey E, Srivastava R, Rosen B, Hyman B. Neurochemical and histologic characterization of striatal excitotoxic lesions produced by the mitochondrial toxin 3-nitropropionic acid. J. Neurosci. 1993;13:4181-4192.

Bossy-Wetzel E, Schwarzenbacher R, Lipton S. Molecular pathways to neurodegeneration. Nat. Med. 2004;10 Suppl.:S2-S9.

Brown R, Lockwood A, Sonawane B. Neurodegenerative diseases: an overview of environmental risk factors. Environ. Health Perspect. 2005;113:1250-1256.

Butterworth J. Changes in nine enzyme markers for neurons, glia, and endothelial cells in agonal state and Huntington's disease caudate nucleus. J. Neurochem. 1986;47:583-587.

Carter C. Loss of glutamine synthetase activity in the brain in Huntington's disease. Lancet 1981;1:782-783.

Chiang M, Chen H, Lee Y, Chang H, Wu Y, Soong B, Chen C, Wu Y, Liu C, Niu D, et al. Dysregulation of C/EBPalpha by mutant Huntingtin causes the urea cycle deficiency in Huntington's disease. Hum. Mol. Genet. 2007;16:483-498.

Choi CJ, Anantharam V, Martin DP, Nicholson EM, Richt JA, Kanthasamy A, Kanthasamy AG. Manganese upregulates cellular prion protein and contributes to altered stabilization and proteolysis: relevance to role of metals in pathogenesis of prion disease. Toxicol. Sci. 2010;115:535-546.

Choi CJ, Anantharam V, Saetveit NJ, Houk RS, Kanthasamy A, Kanthasamy AG. Normal cellular prion protein protects against manganese-induced oxidative stress and apoptotic cell death. Toxicol. Sci. 2007;98:495-509.

Choi CJ, Kanthasamy A, Anantharam V, Kanthasamy AG. Interaction of metals with prion protein: possible role of divalent cations in the pathogenesis of prion diseases. Neurotoxicology 2006;27:777-787.

Coppede F, Mancuso M, Siciliano G, Migliore L, Murri L. Genes and the environment in neurodegeneration. Biosci. Rep. 2006;26:341-367.

Curtis A, Fey C, Morris C, Bindoff L, Ince P, Chinnery P, Coulthard A, Jackson M, Jackson A, McHale D, et al. Mutation in the gene encoding ferritin light polypeptide causes dominant adult-onset basal ganglia disease. Nat. Genet. 2001;28:350-354.

Damiano M, Galvan L, Déglon N, Brouillet E. Mitochondria in Huntington's disease. Biochim. Biophys. Acta 2010;1802:52-61.

Dexter D, Carayon A, Javoy-Agid F, Agid Y, Wells F, Daniel S, Lees A, Jenner P, Marsden C. Alterations in the levels of iron, ferritin and other trace metals in Parkinson's disease and other neurodegenerative diseases affecting the basal ganglia. Brain 1991;114(Pt 4):1953-1975.

Ehrich M, Sharova L. In vitro methods for detecting cytotoxicity. Curr. Protoc. Toxicol. 2000;3:6.2.11-6.2.12.

Eid T, Williamson A, Lee T, Petroff O, de Lanerolle N. Glutamate and astrocytes—key players in human mesial temporal lobe epilepsy? Epilepsia 2008;49 Suppl. 2:42-52.

Ensunsa J, Symons J, Lanoue L, Schrader H, Keen C. Reducing arginase activity via dietary manganese deficiency enhances endothelium-dependent vasorelaxation of rat aorta. Exp. Biol. Med. 2004;229:1143-1153.

Erikson K, Aschner M. Increased manganese uptake by primary astrocyte cultures with altered iron status is mediated primarily by divalent metal transporter. Neurotoxicology 2006;27:125-130.

Erikson K, Shihabi Z, Aschner J, Aschner M. Manganese accumulates in iron-deficient rat brain regions in a heterogeneous fashion and is associated with neurochemical alterations. Biol. Trace Elem. Res. 2002;87:143-156.

Erikson K, Syversen T, Steinnes E, Aschner M. Globus pallidus: a target brain region for divalent metal accumulation associated with dietary iron deficiency. J. Nutr. Biochem. 2004;15:335-341.

Fernandes H, Baimbridge K, Church J, Hayden M, Raymond L. Mitochondrial sensitivity and altered calcium handling underlie enhanced NMDA-induced apoptosis in YAC128 model of Huntington's disease. J. Neurosci. 2007;27:13614-13623.

Firdaus W, Wyttenbach A, Giuliano P, Kretz-Remy C, Currie R, Arrigo A. Huntingtin inclusion bodies are iron-dependent centers of oxidative events. FEBS J. 2006;273:5428-5441.

Fitsanakis V, Zhang N, Anderson J, Erikson K, Avison M, Gore J, Aschner M. Measuring brain manganese and iron accumulation in rats following 14 weeks of low-dose manganese treatment using atomic absorption spectroscopy and magnetic resonance imaging. Toxicol. Sci. 2008;103:116-124.

Fleming M, Romano M, Su M, Garrick L, Garrick M, Andrews N. Nramp2 is mutated in the anemic Belgrade (b) rat: Evidence of a role for Nramp2 in endosomal iron transport. Proc. Natl. Acad. Sci. U.S.A. 1998;95:1148-1153.

Fox JH, Kama JA, Lieberman G, Chopra R, Dorsey K, Chopra V, Volitakis I, Cherny RA, Bush AI, Hersch S. Mechanisms of copper ion mediated Huntington's disease progression. PLoS One 2007;2:e334.

Garcia S, Gellein K, Syversen T, Aschner M. A manganese-enhanced diet alters brain metals and transporters in the developing rat. Toxicol. Sci. 2006;92:516-525.

Garcia S, Gellein K, Syversen T, Aschner M. Iron deficient and manganese supplemented diets alter metals and transporters in the developing rat brain. Toxicol. Sci. 2007;95:205-214.

Girijashanker K, He L, Soleimani M, Reed J, Li H, Liu Z, Wang B, Dalton T, Nebert D. Slc39a14 gene encodes ZIP14, a metal/bicarbonate symporter: similarities to the ZIP8 transporter. Mol. Pharmacol. 2008;73:1413-1423.

Gitler AD, Chesi A, Geddie ML, Strathearn KE, Hamamichi S, Hill KJ, Caldwell KA, Caldwell GA, Cooper AA, Rochet J-C, et al. Alpha-synuclein is part of a diverse and highly conserved interaction network that includes PARK9 and manganese toxicity. Nat. Genet. 2009;41:308-315.

Goytain A, Hines RM, Quamme GA. Huntingtin-interacting proteins, HIP14 and HIP14L, mediate dual functions, palmitoyl acyltransferase and Mg2+ transport. J. Biol. Chem. 2008;283:33365-33374.

Graham R, Deng Y, Slow E, Haigh B, Bissada N, Lu G, Pearson J, Shehadeh J, Bertram L, Murphy Z, et al. Cleavage at the caspase-6 site is required for neuronal dysfunction and degeneration due to mutant huntingtin. Cell 2006;125:1179-1191.

Graham R, Pouladi M, Joshi P, Lu G, Deng Y, Wu N, Figueroa B, Metzler M, Andre V, Slow E, et al. Differential susceptibility to excitotoxic stress in YAC128 mouse models of Huntington disease between initiation and progression of disease. J. Neurosci. 2009;29:2193-2204.

Greger J. Nutrition versus toxicology of manganese in humans: evaluation of potential biomarkers. Neurotoxicology 1999;20:205-212.

Gunshin H, Allerson C, Polycarpou-Schwarz M, Rofts A, Rogers J, Kishi F, Hentze M, Rouault T, Andrews N, Hediger M. Iron-dependent regulation of the divalent metal ion transporter. FEBS Lett. 2001;509:309-316.

Gunshin H, Mackenzie B, Berger U, Gunshin Y, Romero M, Boron W, Nussberger S, Gollan J, Hediger M. Cloning and characterization of a mammalian proton-coupled metal-ion transporter. Nature 1997;388:482-488.

He L, Girijashanker K, Dalton T, Reed J, Li H, Soleimani M, Nebert D. ZIP8, member of the solute-carrier-39 (SLC39) metal-transporter family: characterization of transporter properties. Mol. Pharmacol. 2006;70:171-180.

Heng MY, Detloff PJ, Wang PL, Tsien JZ, Albin RL. In vivo evidence for NMDA receptor-mediated excitotoxicity in a murine genetic model of Huntington disease. J. Neurosci. 2009;29:3200-3205.

Hilditch-Maguire P, Trettel F, Passani L, Auerbach A, Persichetti F, MacDonald M. Huntingtin: an iron-regulated protein essential for normal nuclear and perinuclear organelles. Hum. Mol. Genet. 2000;9:2789-2797.

Keefer RC, Barak AJ, Boyett JD. Binding of manganese and transferrin in rat serum. Biochim. Biophys. Acta 1970;221:390-393.

Kreutz C, Bartolome Rodriguez M, Maiwald T, Seidl M, Blum H, Mohr L, Timmer J. An error model for protein quantification. Bioinformatics 2007;23:2747-2753.

Kwik-Uribe C, Reaney S, Zhu Z, Smith D. Alterations in cellular IRP-dependent iron regulation by in vitro manganese exposure in undifferentiated PC12 cells. Brain Res. 2003;973:1-15.

Kwik-Uribe C, Smith D. Temporal responses in the disruption of iron regulation by manganese. J. Neurosci. Res. 2006;83:1601-1610.

Lee P, Gelbart T, West C, Halloran C, Beutler E. The human Nramp2 gene: characterization of the gene structure, alternative splicing, promoter region and polymorphisms. Blood Cells Mol. Dis. 1998;24:199-215.

Li G, Zhao Q, Zheng W. Alteration at translational but not transcriptional level of transferrin receptor expression following manganese exposure at the blood-CSF barrier in vitro. Toxicol. Appl. Pharmacol. 2005;205:188-200.

Liuzzi JP, Aydemir F, Nam H, Knutson MD, Cousins RJ. Zip14 (Slc39a14) mediates non-transferrin-bound iron uptake into cells. Proc. Natl. Acad. Sci. U.S.A. 2006;103:13612-13617.

Lu L, Zhang L, Li G, Guo W, Liang W, Zheng W. Alteration of serum concentrations of manganese, iron, ferritin, and transferrin receptor following exposure to welding fumes among career welders. Neurotoxicology 2005;26:257-265.

Lumsden A, Henshall T, Dayan S, Lardelli M, Richards R. Huntingtin-deficient zebrafish exhibit defects in iron utilization and development. Hum. Mol. Genet. 2007;16:1905-1920.

Malecki EA, Cook BM, Devenyi AG, Beard JL, Connor JR. Transferrin is required for normal distribution of 59Fe and 54Mn in mouse brain. J. Neurol. Sci. 1999;170:112-118.

Milatovic D, Zaja-Milatovic S, Gupta RC, Yu Y, Aschner M. Oxidative damage and neurodegeneration in manganese-induced neurotoxicity. Toxicol. Appl. Pharmacol. 2009;240:219-225.

Molina-Holgado F, Hider R, Gaeta A, Williams R, Francis P. Metals ions and neurodegeneration. Biometals 2007;20:639-654.

Roze E, Saudou F, Caboche J. Pathophysiology of Huntington's disease: from huntingtin functions to potential treatments. Curr. Opin. Neurol. 2008;21:497-503.

Shin J, Fang Z, Yu Z, Wang C, Li S, Li X. Expression of mutant huntingtin in glial cells contributes to neuronal excitotoxicity. J. Cell Biol. 2005;171:1001-1012.

Simmons D, Casale M, Alcon B, Pham N, Narayan N, Lynch G. Ferritin accumulation in dystrophic microglia is an early event in the development of Huntington's disease. Glia 2007;55:1074-1084.

Stoy N, Mackay G, Forrest C, Christofides J, Egerton M, Stone T, Darlington L. Tryptophan metabolism and oxidative stress in patients with Huntington's disease. J. Neurochem. 2005;93:611-623.

Strand AD, Baquet ZC, Aragaki AK, Holmans P, Yang L, Cleren C, Beal MF, Jones L, Kooperberg C, Olson JM, et al. Expression profiling of Huntington's disease models suggests that brain-derived neurotrophic factor depletion plays a major role in striatal degeneration. J. Neurosci. 2007;27:11758-11768.

Tholey G, Ledig M, Kopp P, Sargentini-Maier L, Leroy M, Grippo AA, Wedler FC. Levels and sub-cellular distribution of physiologically important metal ions in neuronal cells cultured from chick embryo cerebral cortex. Neurochem. Res. 1988a;13:1163-1167.

Tholey G, Ledig M, Mandel P, Sargentini L, Frivold AH, Leroy M, Grippo AA, Wedler FC. Concentrations of physiologically important metal ions in glial cells cultured from chick cerebral cortex. Neurochem. Res. 1988b;13:45-50.

Trettel F, Rigamonti D, Hilditch-Maguire P, Wheeler V, Sharp A, Persichetti F, Cattaneo E, MacDonald M. Dominant phenotypes produced by the HD mutation in STHdh(Q111) striatal cells. Hum. Mol. Genet. 2000;9:2799-2809.

Walker F. Huntington's disease. Lancet 2007;369:218-228.

Wang X, Miller D, Zheng W. Intracellular localization and subsequent redistribution of metal transporters in a rat choroid plexus model following exposure to manganese or iron. Toxicol. Appl. Pharmacol. 2008;230:167-174.

Wedler F, Vichnin M, Ley B, Tholey G, Ledig M, Copin J. Effects of Ca(II) ions on Mn(II) dynamics in chick glia and rat astrocytes: potential regulation of glutamine synthetase. Neurochem. Res. 1994;19:145-151.

Williams BB, Li D, Wegrzynowicz M, Vadodaria BK, Anderson JG, Kwakye GF, Aschner M, Erikson KM, Bowman AB. Disease-toxicant screen reveals a neuroprotective interaction between Huntington's disease and manganese exposure. J. Neurochem. 2010;112:227-237.

Wright RO, Baccarelli A. Metals and neurotoxicology. J. Nutr. 2007;137:2809-2813.

Yin Z, Jiang H, Lee E-S Y, Ni M, Erikson KM, Milatovic D, Bowman AB, Aschner M. Ferroportin is a manganese-responsive protein that decreases manganese cytotoxicity and accumulation. J. Neurochem. 2010;112:1190-1198.

Zeron M, Chen N, Moshaver A, Lee A, Wellington C, Hayden M, Raymond L. Mutant huntingtin enhances excitotoxic cell death. Mol. Cell Neurosci. 2001;17:41-53.

Zhang H, Li Q, Graham R, Slow E, Hayden M, Bezprozvanny I. Full length mutant huntingtin is required for altered Ca2+ signaling and apoptosis of striatal neurons in the YAC mouse model of Huntington's disease. Neurobiol. Dis. 2008;31:80-88.

Zheng W, Zhao Q. Iron overload following manganese exposure in cultured neuronal, but not neuroglial cells. Brain Res. 2001;897:175-179.

Zheng W, Zhao Q, Slavkovich V, Aschner M, Graziano J. Alteration of iron homeostasis following chronic exposure to manganese in rats. Brain Res. 1999;833:125-132.

Zuccato C, Ciammola A, Rigamonti D, Leavitt B, Goffredo D, Conti L, MacDonald M, Friedlander R, Silani V, Hayden M, et al. Loss of huntingtin-mediated BDNF gene transcription in Huntington's disease. Science 2001;293:493-498.

Zuccato C, Liber D, Ramos C, Tarditi A, Rigamonti D, Tartari M, Valenza M, Cattaneo E. Progressive loss of BDNF in a mouse model of Huntington's disease and rescue by BDNF delivery. Pharmacol. Res. 2005;52:133-139.